NANO LETTERS

pubs.acs.org/NanoLett

Letter

Metamaterial Enhancement of Metal-Halide Perovskite Luminescence

Giorgio Adamo,* Harish Natarajan Swaha Krishnamoorthy, Daniele Cortecchia, Bhumika Chaudhary, Venkatram Nalla, Nikolay I. Zheludev, and Cesare Soci*

Cite This: *Nano Lett.* 2020, 20, 7906–7911

Read Online

ACCESS | Metrics & More | Article Recommendations | Supporting Information

ABSTRACT: Metal-halide perovskites are rapidly emerging as solution-processable optical materials for light-emitting applications. Here, we adopt a plasmonic metamaterial approach to enhance photoluminescence emission and extraction of methylammonium lead iodide ($MAPbI_3$) thin films based on the Purcell effect. We show that hybridization of the active metal-halide film with resonant nanoscale sized slits carved into a gold film can yield more than 1 order of magnitude enhancement of luminescence intensity and nearly 3-fold reduction of luminescence lifetime corresponding to a Purcell enhancement factor of more than 300. These results show the effectiveness of resonant nanostructures in controlling metal-halide perovskite light emission properties over a tunable spectral range, a viable approach toward highly efficient perovskite light-emitting devices and single-photon emitters

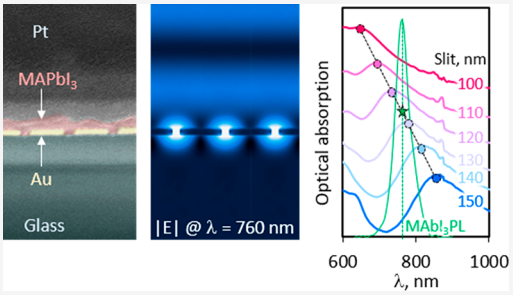

KEYWORDS: *hybrid perovskites, resonant metasurfaces, plasmonic luminescence enhancement, Purcell effect*

Efficient nanoscale light sources are key elements for the development of advanced nanophotonic circuits and integrated thin-film optoelectronic devices. Thanks to their exceptional optoelectronic properties, hybrid organic–inorganic perovskites are gaining prominence for solid-state lighting and displays.[1−4] Limiting factors to the adoption of perovskites in photonic applications are stability[5] and low luminescence yield (low efficiency and relatively slow rate of spontaneous emission), which so far hindered the realization of perovskite-based high-speed light-emitting devices.[6,7] A number of approaches have been adopted to overcome the luminescence yield limitation, ranging from micro/nanostructuring of the perovskite materials[8−13] to distributed feedback and microring lasing cavities.[14−19] Thanks to their ability of trapping, confining, and enhancing the optical fields in nanoscale volumes, plasmonic and dielectric metamaterials have proven to be an excellent platform for the enhancement of both linear and nonlinear properties of media[14,20] and have been used with great success for multifold enhancement of luminescence in variety of active materials like quantum dots, quantum wells, and dyes and ultimately enabling both lasing and spasing.[21−26] Here we exploit the design flexibility of plasmonic metamaterials to alter the luminescence of archetypical $MAPbI_3$ perovskite films hybridized with planar resonant nanoslits tailored to match their emission peak around 760 nm. We control the degree of photoluminescence enhancement by shifting the metamaterial resonance across the $MAPbI_3$ emission line and obtain more than 1 order of magnitude increase in light radiation from the perovskite film; correspondingly, we observe a significant narrowing of the luminescence line width and almost 3-fold reduction of the lifetime. These findings prove that hybridization of metal-halide perovskites with metamaterials could lead to the realization of more efficient and faster nanoscale integrated light-emitting devices and lasers, as well as to the improvement of intrinsic radiative properties of perovskite compounds through the control of light-matter interactions at the nanoscale.

We selected a basic metamaterial design, a periodic array of nanoscale slits carved onto a continuous metallic film, which supports dipolar resonances in the visible spectral range whose wavelength is determined by the slit length. Six metamaterial nanoslit arrays (30 × 30 μm^2 squares) were fabricated by focused ion beam (FIB) milling of a $h_{Au} \approx 30$ nm thin gold layer, evaporated over a glass substrate. The arrays feature an increasing slit length L, ranging from 100–150 nm, in steps of 10 nm, a constant slit width $W \approx 35$ nm, and a square lattice periodicity of $P = 2L$. Figure 1a–c shows secondary electron images of three arrays with slits length $L = 100$ nm (Figure 1a), 120 nm (Figure 1b) and 140 nm (Figure 1c) captured over an ~750 × 750 nm^2 field of view: they are presented side by side

Received: June 20, 2020
Revised: October 16, 2020
Published: October 22, 2020

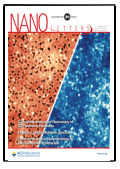

https://dx.doi.org/10.1021/acs.nanolett.0c02571
Nano Lett. 2020, 20, 7906–7911

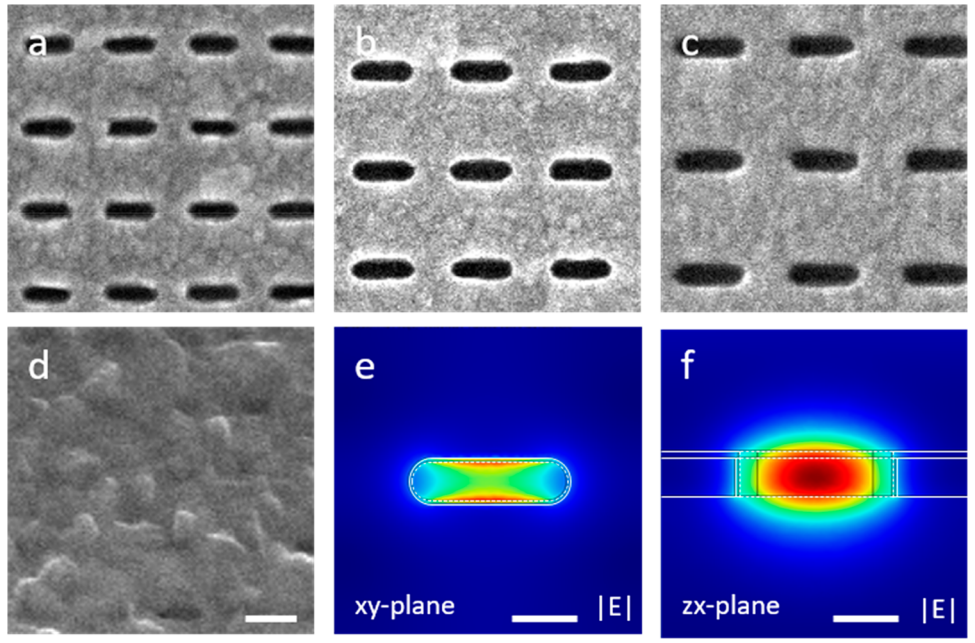

Figure 1. (a–c) Secondary electrons images of slit metamaterials with slit length of, respectively, 100, 120, and 140 nm carved by FIB milling of a 30 nm Au + 5 nm SiO_2 film on glass substrate. (d) Secondary electron image of a 150 nm slit metamaterial coated with 65 nm thick $MAPbI_3$ perovskite film; scale bar is 100 nm. (e,f) Top-view and cross-section maps of the electric field maps at resonance for a 120 nm long slit illuminated by 760 nm light polarized along *y*, showing local field enhancement inside, and in the vicinity of the slit; the scale bar is 50 nm.

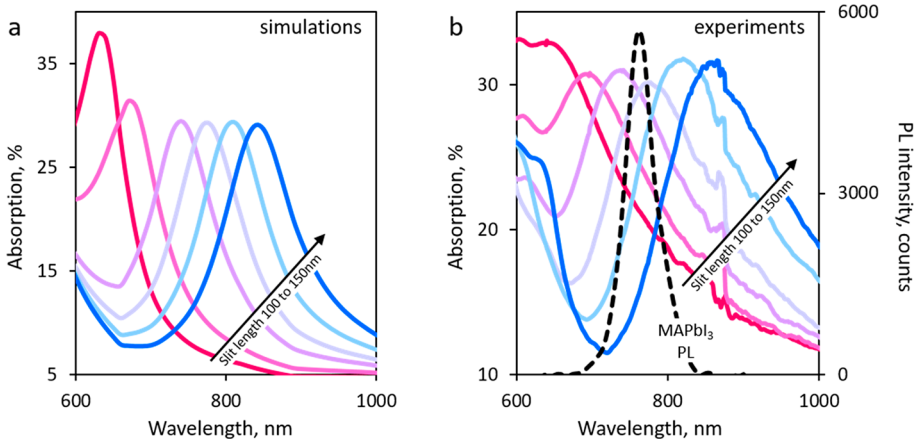

Figure 2. (a) Simulated optical absorption resonance spectra for slit metamaterials with length varying from 100 to 150 nm, in 10 nm steps (magenta to blue lines). (b) Experimental optical absorption resonance spectra for slit metamaterials with length varying from 100 to 150 nm, in 10 nm steps, overlaid with photoluminescence emission spectrum of a 65 nm thick $MAPbI_3$ perovskite film on glass (dashed black line).

to produce a distinct perception of the increase in length and periodicity.

The $MAPbI_3$ precursor solution was spin-coated over the entire nanostructured sample, resulting in a $h_{MAPbI3} \approx 65$ nm thin film with typical roughness of <10 nm, covering both the metamaterials (Figure 1d), the flat gold, and a nearby patch exposing the glass substrate, to ensure as uniform as possible coating conditions for the arrays and the reference areas (see Figure S1 and S2 of Supporting Information). To avoid direct contact between gold and the perovskite film, thus preventing luminescence quenching and the possibility of gold diffusion into the perovskite,[27] an ∼5 nm SiO_2 layer was thermally evaporated onto the sample before spin-coating the $MAPbI_3$ solution. Three-dimensional full-wave electromagnetic simulations confirm the dipolar nature of the resonant field trapped inside the nanoslits and the enhancement of the field intensity and local density of states (LDOS), as shown in Figure 1e,f, respectively.

The photoluminescence spectrum of the $MAPbI_3$ perovskite film peaks around the optical bandgap energy of ∼1.62 eV with relatively narrow full width at half-maximum (fwhm) of ∼50 nm. Figure 2a,b shows the simulated and experimentally measured optical absorption spectra of the different nanoslit metamaterial arrays fabricated for normally incident light with polarization perpendicular to the slits (TM) before spin-coating the perovskite film. The bare metamaterial spectra feature well-pronounced absorption resonances at progressively longer wavelengths with increasing slit length and crossing over the $MAPbI_3$ photoluminescence spectrum at 760 nm (Figure 2b).

The experimental optical spectra of the metamaterials were measured under normal incidence illumination, using a

https://dx.doi.org/10.1021/acs.nanolett.0c02571
Nano Lett. 2020, 20, 7906–7911

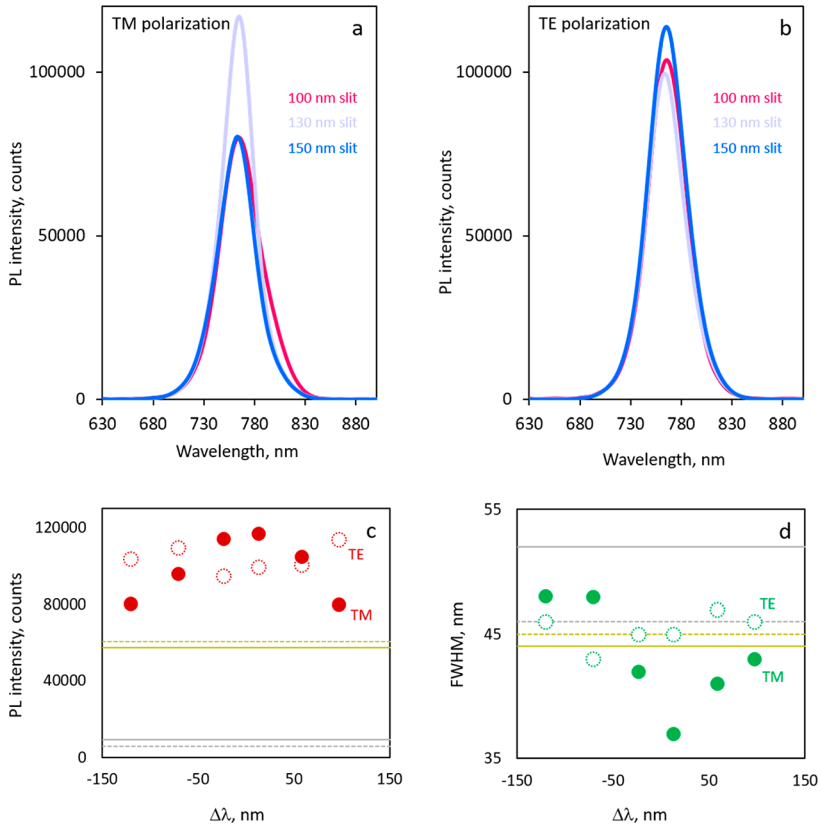

Figure 3. TM (a) and (b) TE (b) polarized spectra of a 65 nm thick $MAPbI_3$ perovskite film on metamaterials with slit lengths of 100 nm (magenta), 130 nm (lilac), and 150 nm (blue). $MAPbI_3$ intensity (c) and line width (d) dependence as a function of the wavelength mismatch between the metamaterial optical absorption resonance and the perovskite emission peak for both TM (full markers) and TE (dashed markers) polarizations (as reference, the horizontal lines indicate the intensities in TM (full lines) and TE (dashed lines) polarizations for the $MAPbI_3$ film on glass (gray) and on gold (gold yellow)).

microphotospectrometer with a circular collection aperture of 25 μm diameter, which allowed removing edge effects from the metamaterial arrays. The simulated spectra were obtained by three-dimensional full-wave electromagnetic simulations using standard literature data for gold[28] and glass.[29] It should be noted that in this spectral interval optical absorption of gold is low (4.5%), therefore the optical fields are mostly trapped within the slits or within the air/glass in its vicinity (Figure 1e,f), thus allowing strong interaction with the overlying perovskite film.

The effect of the nanoslit gold metamaterials on the light emission properties of $MAPbI_3$ perovskite films was evaluated by measuring both steady-state and transient photoluminescence in three configurations: $MAPbI_3$ film on glass, $MAPbI_3$ film on gold (with ~5 nm SiO_2 spacer) and $MAPbI_3$ film on each of the six nanoslit metamaterial arrays (with ~5 nm SiO_2 spacer). In the steady-state measurements, we excited the perovskite film using a picosecond pulsed diode laser and measured the emitted light with a scanning monochromator spectrometer, while time-resolved measurements were performed using an ~100 fs optical parametric oscillator (OPA) as pump and a streak-camera to record the photoluminescence. We have chosen an excitation wavelength of λ = 405 nm, detuned from the metamaterials' resonance, and focused the laser beam to a spot size of about 15 μm to avoid any direct effect of the pump on the interaction between $MAPbI_3$ emission and the nanoslits's resonances. All samples were pumped through the MAPbI3 perovskite film with photoluminescence collected from the same side. In the case of metamaterials, observation from the opposite side would yield greater enhancement;[22] however, we opted for a measuring configuration that is more representative of the enhancement expected in multilayered electroluminescent devices, with light emitted across the film thickness and collected from the transparent bottom contacts.

The steady-state results indicate that the photoluminescence of the $MAPbI_3$ perovskite film is strongly enhanced by the interaction with the metamaterials and that the degree of enhancement can be controlled by the design of the nanoslit's resonators. The measurements were performed selecting the polarization of the emitted light, whereas the polarization of the pump light was left unchanged since both the gold metamaterial and the perovskite film are polarization independent at this wavelength.

Figure 3a,b shows the photoluminescence intensity of the perovskite film on metamaterials for arrays whose resonance is blue-shifted (100 nm slit, magenta curve), centered (130 nm slit, lilac curve), and red-shifted (150 nm slit, blue curve) with respect to the $MAPbI_3$ emission peak in TM (perpendicular to slits) and TE (parallel to slits) polarizations, respectively. It is quite evident that in TM polarization, the photoluminescence intensity is highest when the metamaterial resonance and the perovskite emission peaks match, whereas in TE polarization there is no clear dependence on the metamaterial resonance wavelength. To visualize how the photoluminescence intensity depends on the wavelength mismatch ($\Delta\lambda$) between the

https://dx.doi.org/10.1021/acs.nanolett.0c02571
Nano Lett. 2020, 20, 7906−7911

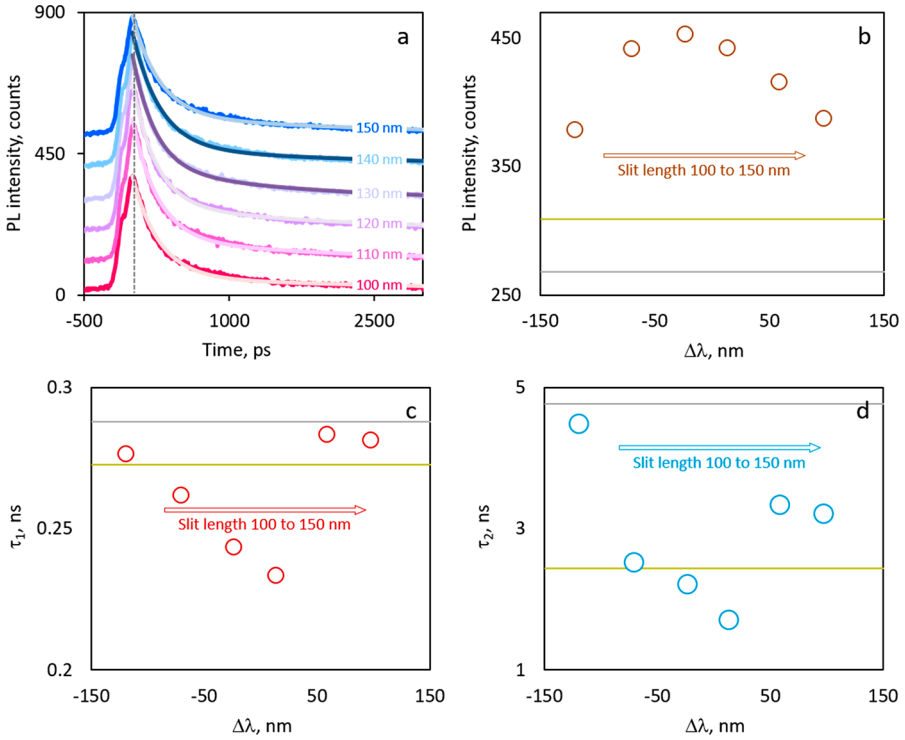

Figure 4. (a) Time-resolved photoluminescence of a 65 nm thick $MAPbI_3$ perovskite film on metamaterials with slit lengths varying from 100 to 160 nm and fitting curves overlaid (spectra are vertically shifted for ease of visualization). Time-resolved photoluminescence peak intensity (b) and two-exponential fitting time dependence (c,d) of $MAPbI_3$ on metamaterials as a function of the detuning of the metamaterial resonance from the perovskite emission peak (as reference, the horizontal lines indicate the PL intensities for the $MAPbI_3$ film on glass (gray) and on gold (gold yellow)).

nanoslits resonance and the $MAPbI_3$ emission, we plot in Figure 3c the photoluminescence peak intensity for (i) the $MAPbI_3$ film on glass (black horizontal lines), (ii) the $MAPbI_3$ film on gold/SiO_2 (yellow horizontal lines), and (iii) the $MAPbI_3$ film on all the six nanoslit metamaterial arrays (red circles), in both TM (full circles) and TE polarization (dashed circles). The following observations can be made: (i) the $MAPbI_3$ photoluminescence intensity increases (~6×) when the film is placed in the vicinity of gold; (ii) the $MAPbI_3$ photoluminescence intensity is further enhanced, by more than 1 order of magnitude (~12×), when the film is placed on the metamaterial slits; (iii) TM polarized photoluminescence shows a clear dependence on $\Delta\lambda$, whereas TE polarized photoluminescence is unaffected by the mismatch between the metamaterial optical absorption resonance and the perovskite emission peak wavelengths. This indicates that resonant nanoslits cause a Purcell enhancement of the photoluminescence by confining the electrical field in a nanometric volume when they are excited with polarization perpendicular to the long axis of the slit.[21] Further evidence of the effect induced on the $MAPbI_3$ photoluminescence by the photonic mode's volume confinement is provided by the line width of the TM polarized photoluminescence emission, which decreases proportionally to $\Delta\lambda$, as shown in Figure 3d. The fact that photoluminescence enhancement is comparable for TM and TE polarizations shall be attributed to the nonconformal coverage of the nanoslit volume by the perovskite films, as explained in Figure S3 (Supporting Information). This also suggests that the values reported here are only a lower bound for achievable enhancement factors.[30]

A direct manifestation of the enhancement of radiative emission rates by the Purcell effect is the reduction of photoluminescence lifetimes.[31,32] The photoluminescence decay traces for the $MAPbI_3$ perovskite film on metamaterial arrays with nanoslits of increasing length are plotted in Figure 4a, together with the fitting curves overlaid to the corresponding spectra (the spectra are vertically shifted for ease of visualization). The peak intensities of the decay traces show a clear dependence on $\Delta\lambda$ (Figure 4b), in good agreement with the behavior of steady-state spectra. The photoluminescence of $MAPbI_3$ films on glass shows a double-exponential decay with characteristic lifetimes of $\tau_1 \approx 0.29$ ns and $\tau_2 \approx 4.8$ ns, which are in good agreement with previous assignments to Auger recombination (τ_1) and charge carrier relaxation through band-edge emission (τ_2).[1]

The hybridization of the $MAPbI_3$ film with the nanoslit metamaterials induces a significant reduction of both τ_1 and τ_2 (Figure 4c,d, respectively), consistent with the dependence of photoluminescence intensity and line width on $\Delta\lambda$. The 3-fold shortening of radiative lifetime τ_2 achieved at maximum overlap ($\Delta\lambda \sim 0$, when the metamaterial resonance wavelength matches the $MAPbI_3$ emission peak) corresponds to a Purcell factor of nearly 3. We also observe a slight reduction (~20%) of the Auger recombination lifetimes, τ_1, correlated with the metamaterial resonances, which may be attributed to plasmon-induced hot carrier generation.[33] The Auger recombination in $MAPbI_3$ is usually very efficient compared to spontaneous emission because of the long-range electron−hole diffusion length: the hybridization of $MAPbI_3$ with metamaterials reduces the τ_2/τ_1 ratio from ~17 to ~7, which suggests shortening of the carrier build-up time for population inversion

https://dx.doi.org/10.1021/acs.nanolett.0c02571
Nano Lett. 2020, 20, 7906−7911

in amplified processes (SE provides seed photons for photon cascade and the avalanche in amplified spontaneous emission, ASE), out-competing Auger processes in thin films. Therefore, the Purcell factor reported here shall be considered as a lower bound. If we consider the environment created by the metamaterial equivalent to a nanocavity, we can adopt the conventional definition of the Purcell Factor as $F = \frac{3}{4\pi}\left(\frac{\lambda}{n}\right)^3\frac{Q}{V}$, where Q and V are the quality factor of the absorption resonance and mode volume for the 130 nm slit metamaterial. With λ = 760 nm, n = 2.4 for $MAPbI_3$, Q = 5.6, and $V = L{\cdot}W{\cdot}h_{Au}$, we estimate the Purcell enhancement factor to be F = 317. This is of the same order of magnitude of the enhancement of photoluminescence, F = 12, observed in experiments, which corrected for the fraction of $MAPbI_3$ inside the 130 nm slits, $f = V/P^2h_{MAPbI3}$ corresponds to a factor $F = \mu/f$ = 386. It should also be noted that time-resolved data were acquired for unpolarized emission, while steady-state measurements indicate that nanoslit cavities affect almost exclusively TM polarized photoluminescence. Moreover, all measurements were performed at room temperature, therefore a further increase in radiative rates could be expected at lower temperatures. Thus, the improvements in luminescence properties of perovskite films coupled to resonant metamaterial structures registered so far (enhancement of photoluminescence intensity, narrowing of steady-state line widths, and shortening of SE lifetimes) could arguably lead to a reduction of amplified spontaneous emission (ASE) and lasing thresholds, that is, an important step toward integrated perovskites light-emitting devices.

In summary, inspired by the proven ability of metamaterials to manipulate radiation, promote light-matter interaction, and facilitate emission at any wavelength and across numerous types of media, we hybridized a metal-halide perovskite film with nanoslit gold metamaterials to control and enhance its optical emission. We demonstrated a substantial increase of the intrinsic photoluminescence intensity by more than 1 order of magnitude when the metamaterial resonance was tuned to the perovskite intrinsic emission peak. This increase in photoluminescence intensity is accompanied by a significant reduction in the spontaneous emission lifetimes, clearly indicating that the enhancement is radiative in nature. Improved performance and additional functionalities can be foreseen by optimization of the metamaterial structures and their coupling to the perovskite films (e.g., better permeation of the perovskite precursors into the nanostructured scaffold before conversion and crystallization). Similar design principles could also be adopted in the layout of electrodes.[34] Thus, our strategy hints at potential reductions of amplified spontaneous emission (ASE) and lasing thresholds, paving the way toward on-chip integrated perovskite photonic components with wide spectral tunability from UV to NIR and could potentially constitute a viable architecture for perovskite-based integrated light-emitting devices, both optically and electrically pumped.

■ ASSOCIATED CONTENT

Supporting Information

The Supporting Information is available free of charge at https://pubs.acs.org/doi/10.1021/acs.nanolett.0c02571.

Additional materials including details on device fabrication, optical measurement, steady state photoluminescence, time-resolved photoluminescence and COMSOL simulations (PDF)

■ AUTHOR INFORMATION

Corresponding Authors

Giorgio Adamo − *Centre for Disruptive Photonic Technologies, TPI, SPMS, Nanyang Technological University, Singapore 637371;* orcid.org/0000-0003-1974-3368; Email: G.Adamo@ntu.edu

Cesare Soci − *Centre for Disruptive Photonic Technologies, TPI, SPMS and Energy Research Institute at NTU (ERI@N), Research Techno Plaza, Nanyang Technological University, Singapore 637371;* orcid.org/0000-0002-0149-9128; Email: csoci@ntu.edu.sg

Authors

Harish Natarajan Swaha Krishnamoorthy − *Centre for Disruptive Photonic Technologies, TPI, SPMS, Nanyang Technological University, Singapore 637371;* orcid.org/0000-0001-6107-3383

Daniele Cortecchia − *Energy Research Institute at NTU (ERI@N), Research Techno Plaza and Interdisciplinary Graduate School, Nanyang Technological University, Singapore 6375533;* orcid.org/0000-0001-8623-9191

Bhumika Chaudhary − *Energy Research Institute at NTU (ERI@N), Research Techno Plaza and Interdisciplinary Graduate School, Nanyang Technological University, Singapore 6375533*

Venkatram Nalla − *Centre for Disruptive Photonic Technologies, TPI, SPMS, Nanyang Technological University, Singapore 637371;* orcid.org/0000-0003-4535-290X

Nikolay I. Zheludev − *Centre for Disruptive Photonic Technologies, TPI, SPMS, Nanyang Technological University, Singapore 637371; Optoelectronics Research Centre and Centre for Photonic Metamaterials, University of Southampton, Southampton SO17 1BJ, United Kingdom*

Complete contact information is available at: https://pubs.acs.org/10.1021/acs.nanolett.0c02571

Funding

Singapore Ministry of Education Tier 3 Grant (MOE2016-T3-1-006); Singapore National Research Foundation, Prime Minister's Office under its Competitive Research Programme (CRP Award No. NRF-CRP14−2014-03); A*STAR-AME programmatic grant on Nanoantenna Spatial Light Modulators for Next-Gen Display Technologies (Grant A18A7b0058).

Notes

The authors declare no competing financial interest.

The data that support the findings of this study are openly available in NTU research data repository DR-NTU (Data) at 10.21979/N9/DISCX3.

■ REFERENCES

(1) Xing, G.; Mathews, N.; Lim, S. S.; Yantara, N.; Liu, X.; Sabba, D.; Grätzel, M.; Mhaisalkar, S.; Sum, T. C. Low-temperature solution-processed wavelength-tunable perovskites for lasing. *Nat. Mater.* **2014**, *13*, 476.

(2) Tan, Z.-K.; Moghaddam, R. S.; Lai, M. L.; Docampo, P.; Higler, R.; Deschler, F.; Price, M.; Sadhanala, A.; Pazos, L. M.; Credgington, D.; Hanusch, F.; Bein, T.; Snaith, H. J.; Friend, R. H. Bright light-emitting diodes based on organometal halide perovskite. *Nat. Nanotechnol.* **2014**, *9*, 687.

(3) D'Innocenzo, V.; Srimath Kandada, A. R.; De Bastiani, M.; Gandini, M.; Petrozza, A. Tuning the Light Emission Properties by Band Gap Engineering in Hybrid Lead Halide Perovskite. *J. Am. Chem. Soc.* **2014**, *136*, 17730.

(4) Chin, X. Y.; Cortecchia, D.; Yin, J.; Bruno, A.; Soci, C. Lead iodide perovskite light-emitting transistor. *Nat. Commun.* **2015**, *6*, 7383.
(5) Motti, S. G.; Meggiolaro, D.; Barker, A. J.; Mosconi, E.; Perini, C. A. R.; Ball, J. M.; Gandini, M.; Kim, M.; De Angelis, F.; Petrozza, A. Controlling competing photochemical reactions stabilizes perovskite solar cells. *Nat. Photonics* **2019**, *13*, 532.
(6) Yuan, M.; Quan, L. N.; Comin, R.; Walters, G.; Sabatini, R.; Voznyy, O.; Hoogland, S.; Zhao, Y.; Beauregard, E. M.; Kanjanaboos, P.; Lu, Z.; Kim, D. H.; Sargent, E. H. Perovskite energy funnels for efficient light-emitting diodes. *Nat. Nanotechnol.* **2016**, *11*, 872.
(7) Xing, G.; Wu, B.; Wu, X.; Li, M.; Du, B.; Wei, Q.; Guo, J.; Yeow, E. K. L.; Sum, T. C.; Huang, W. Perovskite energy funnels for efficient light-emitting diodes. *Nat. Commun.* **2017**, *8*, 14558.
(8) Zhang, Q.; Ha, S. T.; Liu, X.; Sum, T. C.; Xiong, Q. Room-Temperature Near-Infrared High-Q Perovskite Whispering-Gallery Planar Nanolasers. *Nano Lett.* **2014**, *14*, 5995.
(9) Gholipour, B.; Adamo, G.; Cortecchia, D.; Krishnamoorthy, H. N. S.; Birowosuto, M. D.; Zheludev, N. I.; Soci, C. Organometallic perovskite metasurfaces. *Adv. Mater.* **2017**, *29*, 1604268.
(10) Pourdavoud, N.; Wang, S.; Mayer, A.; Hu, T.; Chen, Y.; Marianovich, A.; Kowalsky, W.; Heiderhoff, R.; Scheer, H.-C.; Riedl, T. Photonic Nanostructures Patterned by Thermal Nanoimprint Directly into Organo-Metal Halide Perovskites. *Adv. Mater.* **2017**, *29*, 1605003.
(11) Makarov, S. V.; Milichko, V.; Ushakova, E. V.; Omelyanovich, M.; Pasaran, A. C.; Haroldson, R.; Balachandran, B.; Wang, H.; Hu, W.; Kivshar, Y. S.; Zakhidov, A. A. Multifold Emission Enhancement in Nanoimprinted Hybrid Perovskite Metasurfaces. *ACS Photonics* **2017**, *4*, 728.
(12) Tiguntseva, E. Y.; Zograf, G. P.; Komissarenko, F. E.; Zuev, D. A.; Zakhidov, A. A.; Makarov, S. V.; Kivshar, Y. S. Light-Emitting Halide Perovskite Nanoantennas. *Nano Lett.* **2018**, *18*, 1185.
(13) Berestennikov, A. S.; Voroshilov, P. M.; Makarov, S. V.; Kivshar, Y. S. Active meta-optics and nanophotonics with halide perovskites. *Appl. Phys. Rev.* **2019**, *6*, No. 031307.
(14) Jia, Y.; Kerner, R. A.; Grede, A. J.; Brigeman, A. N.; Rand, B. P.; Giebink, N. C. Diode-Pumped Organo-Lead Halide Perovskite Lasing in a Metal-Clad Distributed Feedback Resonator. *Nano Lett.* **2016**, *16*, 4624.
(15) Zhang, H.; Liao, Q.; Wu, Y.; Zhang, Z.; Gao, Q.; Liu, P.; Li, M.; Yao, J.; Fu, H. 2D Ruddlesden−Popper Perovskites Microring Laser Array. *Adv. Mater.* **2018**, *30*, 1706186.
(16) Cegielski, P. J.; Giesecke, A. L.; Neutzner, S.; Porschatis, C.; Gandini, M.; Schall, D.; Perini, C. A. R.; Bolten, J.; Suckow, S.; Kataria, S.; Chmielak, B.; Wahlbrink, T.; Petrozza, A.; Lemme, M. C. Monolithically Integrated Perovskite Semiconductor Lasers on Silicon Photonic Chips by Scalable Top-Down Fabrication. *Nano Lett.* **2018**, *18*, 6915.
(17) Li, Z.; Moon, J.; Gharajeh, A.; Haroldson, R.; Hawkins, R.; Hu, W.; Zakhidov, A.; Gu, Q. Room-Temperature Continuous-Wave Operation of Organometal Halide Perovskite Lasers. *ACS Nano* **2018**, *12*, 10968.
(18) Kim, H.; Roh, K.; Murphy, J. P.; Zhao, L.; Gunnarsson, W. B.; Longhi, E.; Barlow, S.; Marder, S. R.; Rand, B. P.; Giebink, N. C. Optically Pumped Lasing from Hybrid Perovskite Light-Emitting Diodes. *Adv. Opt. Mater.* **2020**, *8*, 1901297.
(19) Pourdavoud, N.; Haeger, T.; Mayer, A.; Cegielski, P. J.; Giesecke, A. L.; Heiderhoff, R.; Olthof, S.; Zaefferer, S.; Shutsko, I.; Henkel, A.; Becker-Koch, D.; Stein, M.; Cehovski, M.; Charfi, O.; Johannes, H.-H.; Rogalla, D.; Lemme, M. C.; Koch, M.; Vaynzof, Y.; Meerholz, K.; Kowalsky, W.; Scheer, H.-C.; Görrn, P.; Riedl, T. Room-Temperature Stimulated Emission and Lasing in Recrystallized Cesium Lead Bromide Perovskite Thin Films. *Adv. Mater.* **2019**, *31*, 1903717.
(20) Nikolaenko, A. E.; De Angelis, F.; Boden, S. A.; Papasimakis, N.; Ashburn, P.; Di Fabrizio, E.; Zheludev, N. I. Carbon nanotubes in a photonic metamaterial. *Phys. Rev. Lett.* **2010**, *104*, 153902.
(21) Lee, J.; Tymchenko, M.; Argyropoulos, C.; Chen, P.-Y.; Lu, F.; Demmerle, F.; Boehm, G.; Amann, M.-C.; Alù, A.; Belkin, M. A. Giant nonlinear response from plasmonic metasurfaces coupled to intersubband transitions. *Nature* **2014**, *511*, 65.
(22) Tanaka, K.; Plum, E.; Ou, J. Y.; Uchino, T.; Zheludev, N. I. Multifold enhancement of quantum dot luminescence in plasmonic metamaterials. *Phys. Rev. Lett.* **2010**, *105*, 227403.
(23) Zhou, W.; Dridi, M.; Suh, J. Y.; Kim, C. H.; Co, D. T.; Wasielewski, M. R.; Schatz, G. C.; Odom, T. W. Lasing action in strongly coupled plasmonic nanocavity arrays. *Nat. Nanotechnol.* **2013**, *8*, 506.
(24) Ha, S. T.; Fu, Y. H.; Emani, N. K.; Pan, Z.; Bakker, R. M.; Paniagua-Domínguez, R.; Kuznetsov, A. I. Directional lasing in resonant semiconductor nanoantenna arrays. *Nat. Nanotechnol.* **2018**, *13*, 1042.
(25) Noginov, M. A.; Zhu, G.; Belgrave, A. M.; Bakker, R.; Shalaev, V. M.; Narimanov, E. E.; Stout, S.; Herz, E.; Suteewong, T.; Wiesner, U. Demonstration of a spaser-based nanolaser. *Nature* **2009**, *460*, 1110.
(26) Hoang, T. B.; Akselrod, G. M.; Argyropoulos, C.; Huang, J.; Smith, D. R.; Mikkelsen, M. H. Ultrafast spontaneous emission source using plasmonic nanoantennas. *Nat. Commun.* **2015**, *6*, 7788.
(27) Domanski, K.; Correa-Baena, J.-P.; Mine, N.; Nazeeruddin, M. K.; Abate, A.; Saliba, M.; Tress, W.; Hagfeldt, A.; Grätzel, M. Not All That Glitters Is Gold: Metal-Migration-Induced Degradation in Perovskite Solar Cells. *ACS Nano* **2016**, *10*, 6306.
(28) Johnson, P. B.; Christy, R. W. Optical constants of the noble metals. *Phys. Rev. B* **1972**, *6*, 4370.
(29) Malitson, I. H. Interspecimen comparison of the refractive index of fused silica. *J. Opt. Soc. Am.* **1965**, *55*, 1205−1208.
(30) Janssen, O. T. A.; Wachters, A. J. H.; Urbach, H. P. Efficient optimization method for the light extraction from periodically modulated LEDs using reciprocity. *Opt. Express* **2010**, *18*, 24522.
(31) Koenderink, A. F. On the use of Purcell factors for plasmon antennas. *Opt. Lett.* **2010**, *35*, 4208.
(32) Rose, A.; Hoang, T. B.; McGuire, F.; Mock, J. J.; Ciracì, C.; Smith, D. R.; Mikkelsen, M. H. Control of radiative processes using tunable plasmonic nanopatch antennas. *Nano Lett.* **2014**, *14*, 4797.
(33) Brongersma, M. L.; Halas, N. J.; Nordlander, P. Plasmon-induced hot carrier science and technology. *Nat. Nanotechnol.* **2015**, *10*, 25.
(34) Esfandyarpour, M.; Curto, A. G.; Kik, P. G.; Engheta, N.; Brongersma, M. Optical emission near a high-impedance mirror. *Nat. Commun.* **2018**, *9*, 3224.

https://dx.doi.org/10.1021/acs.nanolett.0c02571
Nano Lett. 2020, 20, 7906−7911